European Journal of Applied Physiology (2019) 119:2201–2213
https://doi.org/10.1007/s00421-019-04204-8

ORIGINAL ARTICLE

P_i-induced muscle fatigue leads to near-hyperbolic power–duration dependence

Bernard Korzeniewski[1]

Received: 12 March 2019 / Accepted: 1 August 2019 / Published online: 9 August 2019

Abstract

Purpose Consequences of combining three ideas proposed previously by other authors: (1) that there exists a critical power (CP), above which no steady state in $\dot{V}O_2$ (oxygen consumption) and metabolites can be achieved in voluntary constant-power exercise; (2) that muscle fatigue is related to decreased exercise efficiency (increased $\dot{V}O_2$/power output ratio); and (3) that P_i (inorganic phosphate) is the main fatigue-related metabolite are investigated.

Methods A previously-developed computer model of the skeletal muscle bioenergetic system is used. It was assumed in computer simulations that skeletal muscle work terminates when cytosolic P_i (inorganic phosphate) exceeds a certain critical level.

Results Simulated changes in muscle $\dot{V}O_2$, cytosolic ADP, pH, PCr and P_i as a function of time at various ATP usage activities (corresponding to power outputs) agreed well with experimental data. Computer simulations resulted in a fourth previously-published idea: (4) that the power–duration relationship describing the dependence of power output (PO) on the time to exhaustion of voluntary constant-power exercise at a given PO has a (near-)hyperbolic shape.

Conclusions P_i is a major factor contributing to muscle fatigue, as such an assumption leads to a (near-)hyperbolic shape of the power–duration relationship, at least for exercise duration of ~ 1–10 min. Thus, a potential mechanism underlying the power–duration relationship shape is offered that was absent in the literature. Other factors/mechanisms, such as cytosol acidification, glycogen stores depletion and central fatigue can contribute to this relationship, especially in longer exercises.

Keywords Muscle fatigue · Power output · Critical power · Exercise duration · Computer model

Abbreviations

A_{UT}	Relative of ATP usage activity
CP	Critical power
OXPHOS	Oxidative phosphorylation
PCr	Phosphocreatine
P_i	Inorganic phosphate
PO	Power output
$\dot{V}O_2$	Oxygen uptake (muscle or pulmonary)

Communicated by Anni Vanhatalo.

✉ Bernard Korzeniewski
bernard.korzeniewski@gmail.com

[1] BioSimulation Center, ul. Filarecka 6/7, 30-110 Kraków, Poland

Introduction

Muscle fatigue can be defined as progressive decline of performance (Allen et al. 2008; Allen and Westerblad 2001) or reduction of muscle force or power for a given muscle activation (Enoka and Duchateau 2008; Grassi et al., 2015). In voluntary exercise it can lead to exercise intolerance = task failure (Grassi et al., 2015).

Peripheral and central fatigue have been distinguished. The former is caused by some intramuscular factors, in particular by changes in myocyte metabolites and pH, decline in signaling factors (Ca^{2+} ions), release of reactive oxygen species (ROS) and/or depletion of glycogen stores (Allen et al. 2008; Wan et al. 2018; Cooke et al. 1988). Several metabolites have been proposed to be related to muscle fatigue, for instance P_i, H^+, ADP, lactate, ATP, Mg^{2+}, etc. Central fatigue is related to a decline of the intensity of neural stimulation of working muscles (Gandevia 2001).

Critical power (CP) is the power output (PO), above which no steady state in $\dot{V}O_2$, cytosolic metabolite concentrations and pH can be achieved (Jones et al. 2010; Poole

et al. 2016). There appears the so-called slow component of the $\dot{V}O_2$ (and metabolites) on-kinetics (Poole et al. 1988; Jones et al. 2010). It was postulated that the slow component is related to the additional ATP usage above CP, underlying the decrease in muscle work efficiency (Rossiter et al. 2002; Rossiter 2011; Jones et al. 2011).

It was proposed that muscle fatigue is related to a decreased exercise efficiency (increased $\dot{V}O_2$/PO ratio), manifesting itself as the slow component of the $\dot{V}O_2$ and metabolites on-kinetics (Grassi et al. 2015). For instance, both phenomena are related to changes in myocyte metabolites and pH.

It was also proposed that P_i is the main fatigue-related metabolite, while a smaller role is played by other metabolites, such as protons (Allen et al. 2008). P_i can inhibit the transition to high-force cross-bridge states and decrease the myofibrillar Ca^{2+} sensitivity. Or, alternatively, P_i could deplete Ca^{2+} ions by precipitating them within sarcoplasmic reticulum (SR) (Allen et al. 2008; Allen and Westerblad 2001). The conceptual benefit of this mechanism is that a small further relative increase in P_i could lead to a complete depletion of remaining free Ca^{2+} ions that constitute the signal for muscle contraction.

It has been demonstrated that the dependence of power output on the duration time of voluntary constant-power exercise of a given power output is well described by a hyperbolic power–duration curve, with critical power as an asymptote, at least in the time range of about 2–15 min (Jones et al. 2010; Poole et al. 2016). However, the mechanisms underlying the hyperbolic shape of the power–duration relationship are unclear.

It has been shown (Korzeniewski and Rossiter 2015), using a computer model of the skeletal muscle bioenergetics system developed previously, that a linear increase in the additional ATP usage with time, assumed to underlie the slow component of the $\dot{V}O_2$ (and metabolites) on-kinetics, gives a good agreement of computer simulations with experimental data concerning time courses of $\dot{V}O_2$, PCr, cytosolic pH as well as the intensity of ATP supply by oxidative phosphorylation, creatine kinase and anaerobic glycolysis during rest–work–recovery transitions in severe knee-extension exercise (Cannon et al. 2014). It has been proposed that the linear increase of the additional ATP usage with time and PO above CP is responsible for the differences in the $\dot{V}O_2$–PO relationship (nonlinearity) in constant-power exercise, step-incremental exercise and ramp-incremental exercise of different slopes (Korzeniewski, 2018b).

The present theoretical study analyses the consequences of the assumption that voluntary constant-power exercise is terminated because of muscle fatigue when P_i concentration exceeds a certain critical value. It is hypothesized that the simulated ATP usage activity–duration relationship, corresponding to the power–duration relationship for a given kind of exercise, will be near-hyperbolic, at least for exercise duration range of about 1.5–10 min tested experimentally. Therefore, it is supposed that the P_i-induced fatigue contributes significantly to the shape of this dependence, although the contribution of other factors, such as pH, glycogen depletion and central fatigue should be also taken into account. Thus, the present study is intended to propose a mechanism underlying the (near-)hyperbolic shape of the power–duration relationship. To the author's knowledge, no such mechanism has been postulated in the literature.

Theoretical methods

Ethical approval

This is a purely theoretical study that did not involve any experiments on humans or animals.

Computer model

The computer model of OXPHOS and the entire bioenergetic system in intact skeletal muscle (Korzeniewski and Zoladz 2001; Korzeniewski and Liguzinski 2004; Korzeniewski and Rossiter 2015; Korzeniewski 2018a, 2018b) was used in the simulations carried out in the present study. This model comprises explicitly the NADH supply block (TCA cycle, fatty-acid β-oxidation, MAS etc.), particular OXPHOS complexes (complex I, complex III, complex IV, ATP synthase, ATP/ADP carrier, and P_i carrier), proton leak through the inner mitochondrial membrane, glycolysis (aerobic and anaerobic), ATP usage, creatine kinase (CK) and proton efflux/influx to/from blood. It involves the so-called each-step activation mechanisms of the regulation of OXPHOS, NADH supply and glycolysis (Korzeniewski 1998; Korzeniewski 2017a). The complete model description is given in "Appendix"and located on the website: https://awe.mol.uj.edu.pl/~benio/.

This model is able to account for numerous, frequently apparently unrelated to each other, kinetic properties and phenomena of the skeletal muscle bioenergetic system during exercise (see Korzeniewski 2017a for a recent review as well as Korzeniewski 2018a, b).

Simulation procedures

The relative activity of ATP usage A_{UT} (relative increase in its rate constant k_{UT} in relation to rest) between 50 (critical A_{UT}, A_{UTcrit}, see below) and 105 (maximum A_{UT}) was used in computer simulations. It was demonstrated that one A_{UT} unit corresponds on average to about 3 W during whole-body exercise, e.g. cycling (Korzeniewski 2018a). However, this

value can vary between, say, 2 W and 4 W, depending, e.g. on body and working muscles mass.

The absolute additional ATP usage activity (rate in mM min^{-1}) is described by the following equation (Korzeniewski 2018a):

$$v_{\mathrm{UTadd}} = k_{\mathrm{UTadd}} \cdot v_{\mathrm{UT}} \cdot \left(A_{\mathrm{UT}} - A_{\mathrm{UTcrit}}\right) \cdot t_{\mathrm{exerc}} \quad (1)$$

where v_{UTadd} (dependent variable) is the absolute additional ATP usage flux (in mM min^{-1}), k_{UTadd} (constant) is the 'rate constant' of the increase in the absolute additional ATP usage in time (in min^{-1}), v_{UT} (dependent variable) is the actual ATP usage flux (in mM min^{-1}), A_{UT} (constant) is the relative ATP usage activity (activation in relation to rest, relative increase in the ATP usage rate constant k_{UT}) (unitless), A_{UTcrit} (constant) is the critical relative ATP usage activity (unitless) and t_{exerc} (independent variable) is time (min) after the onset of exercise. In the simulations carried out in the present study it is assumed that $A_{\mathrm{UTcrit}} = 50$ (unitless) and $k_{\mathrm{UTadd}} = 0.0008$ min^{-1}, as in (Korzeniewski 2018a).

The increase of v_{UTadd} in time was proposed to underlie the continuous increase in $\dot{V}O_2$ in time during exercise with PO > CP, that is the slow component of the $\dot{V}O_2$ on-kinetics (Rossiter 2011; Korzeniewski and Zoladz 2015; Korzeniewski and Rossiter 2015), while the increase in v_{UTadd} with A_{UT} above A_{UTcrit} is assumed due to the fact that the magnitude (slope) of the slow component increases with power output (Murgatroyd et al. 2011; Wilkerson et al. 2004; Burnley and Jones 2007; Özyener et al. 2001; Rossiter 2011).

According to Eq. (1) the additional ATP usage (v_{UTadd}) increases linearly after the onset of exercise both with time and A_{UT} above $A_{\mathrm{UT\,crit}}$ (A_{UT} - A_{UTcrit}). The linear increase in v_{UTadd} with time gives a good agreement of model predictions with experimental data (Korzeniewski and Rossiter 2015). Simulated dependence of the rate of the increase of the additional ATP usage and additional muscle $\dot{V}O_2$ (slope of the slow component of the $\dot{V}O_2$ on-kinetics) at the end of exercise on ATP usage activity (A_{UT}) is compared with experimental dependence of the rate of the increase in the additional pulmonary $\dot{V}O_2$ (slope of the slow component) at the end of exercise on power output extracted from (Murgatroyd et al. 2011) in Fig. 1. A good agreement can be observed. The simulated additional ATP usage increases faster than linearly with ATP usage activity (A_{UT}), as v_{UTadd} depends not only on $A_{\mathrm{UT}} - A_{\mathrm{UTcrit}}$, but also on the absolute flux of ATP usage (v_{UT}) (compare Eq. 1). Therefore, the kinetic expression appearing in Eq. (1) seems well justified by the good agreement with experimental data it produces. This theoretical result further validates the previous computer simulations concerning the muscle $\dot{V}O_2$–PO nonlinearity in constant-power, step-incremental and ramp-incremental exercise of different slope (Korzeniewski 2018b).

The total absolute ATP usage activity A_{UTtot} (in mM min^{-1}) is equal to the sum of the normal and additional absolute ATP usage activity:

$$v_{\mathrm{UTtot}} = v_{\mathrm{UT}} + v_{\mathrm{UTadd}} \quad (2)$$

The rest-to-work transition for voluntary constant-power exercise was simulated as described in Korzeniewski (2018a).

The crucial assumption made in the present study is that muscle work is terminated when P_i concentration reaches the critical value (P_{icrit}) of 25 mM. This is just the maximum P_i concentration in some muscles, although this value can be higher, e.g., 27 mM, in other muscles.

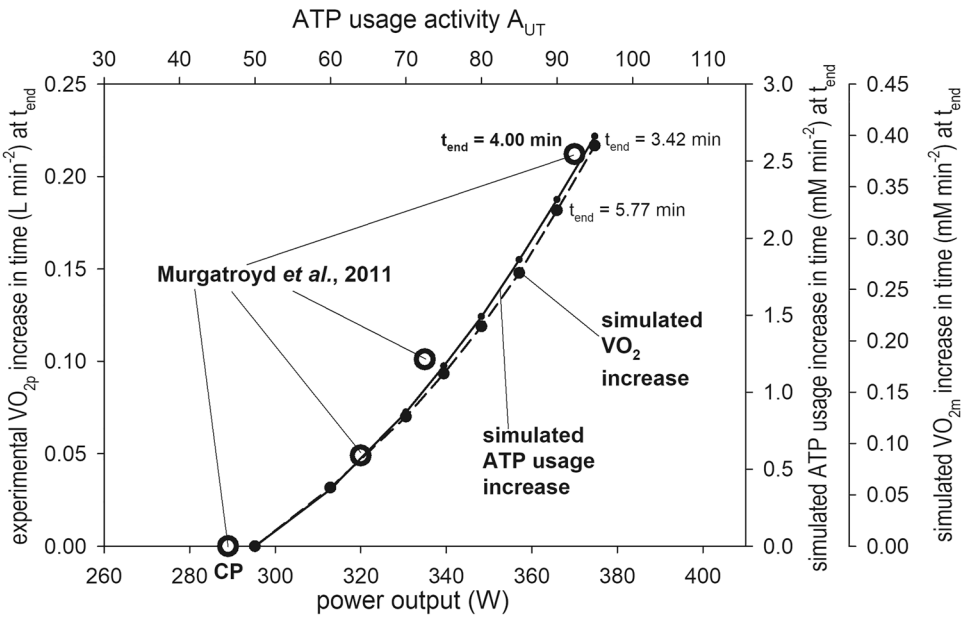

Fig. 1 Comparison of the experimental dependence (open circles) of the rate of pulmonary $\dot{V}O_2$ increase ($\dot{V}O_2$ slow component slope) (left *y* axis) at the time (t_{term}) of the termination of exercise on loaded power output (PO) (lower *x* axis) with the simulated dependence of the rate of muscle $\dot{V}O_2$ increase ($\dot{V}O_2$ slow component slope) (dashed line) (far right *y* axis) and ATP usage activity increase (ATP usage 'slow component' slope) (solid line) (right *y* axis) on ATP usage activity (A_{UT}) (upper *x* axis) at the time (t_{term}) of the termination of exercise. Experimental points were extracted from (Murgatroyd et al. 2011)

Therefore, each simulation, for a given ATP usage activity, was continued until P_i reached 25 mM, and then terminated. Appropriate variable values were recorded at that point. Similar general theoretical results were obtained when the critical P_i level of 27 mM was assumed (not shown). Therefore, the detailed value of critical P_i is of minor importance as long as it is identical for different ATP usage intensities in a given particular case.

Theoretical results

The simulated increase in muscle $\dot{V}O_2$ as a function of time after the onset of voluntary constant-power exercise for various ATP usage activities (A_{UT}) is presented in Fig. 2a. After a quick initial rise, $\dot{V}O_2$ continues to increase with time with a slower pace, the faster, the higher ATP usage activity. Essentially identical $\dot{V}O_2$ is reached in the moment of termination of exercise because of fatigue for ATP usage activities being greater than the critical ATP usage activity.

In computer simulations, ADP increases and pH decreases (after an initial rise) as a function of time after the onset of exercise. The rate of these changes slows down with time, at least for lower ATP usage activities. This is demonstrated in Fig. 2b. The end-exercise ADP and pH are similar, but not identical for various ATP usage activities. The minimum end-exercise ADP and pH values are present at ATP usage activities from 85 to 95, and they are slightly greater both for higher and lower ATP usage activities.

The simulated P_i increases, PCr decreases, while ATP remains essentially constant (no AMP deamination was involved in these simulations) during exercise (Fig. 2c). These changes are very quick at the onset of exercise, and significantly slow down after about 2 min of exercise, being nevertheless faster at higher ATP usage intensities. This is demonstrated in Fig. 2c. The end-exercise PCr and P_i are essentially identical (P_i by definition) for all ATP usage activities.

The simulated relationship between ATP usage activity (A_{UT}) and time to termination of exercise has a near-hyperbolic shape, at least for exercise duration of 1.5–8 (–10) min. This is shown in Fig. 3. This relationship is similar to the experimental power–duration relationship for knee-extension exercise encountered in (Vanhatalo et al. 2010) (Fig. 3). Nevertheless, the simulated ATP usage activity–exercise duration relationship begins to deviate from the hyperbolic fit of experimental points for time longer than about 8–10 min.

The simulated relationship between ATP usage activity (A_{UT}) and the inverse of time (1/time) to termination of exercise is near-linear down to the value of 1/time > 0.12 1/min (time < 8 min). This theoretical result agrees well with experimental data concerning the relationship between power output and time inverse of exercise duration that also is linear. This is demonstrated in Fig. 4, where computer simulations are compared with experimental data concerning constant-power whole-body exercise (cycling): Murgatroy et al. (2011), Wilkerson et al. (2004) and Burnley and Jones (2007). The left and far-left *y* axes are for power outputs in the three sets of experimental data, while the right *y* axis is for the simulated ATP usage activity, proportional within the model to power output for a given exercise type. While a good agreement (near-linear dependence) can be observed between the theoretical curve and experimental points for most of the range of the time inverse presented, the simulated A_{UT} − 1/time dependence starts to deviate from linearity for 1/time < ~0.12 1/min (t > ~8 min).

The theoretical results presented in Figs. 3 and 4 are relatively independent on the assumed values of the critical ATP usage activity A_{UTcrit} and the 'rate constant' (intensity) of the increase in the additional ATP usage activity k_{UTadd} (compare Eq. 1) (not shown).

Discussion

The present theoretical study demonstrates that the assumption that voluntary skeletal muscle work is terminated because of fatigue when the cytosolic inorganic phosphate (P_i) concentration exceeds a certain critical value results in a near-hyperbolic dependence of ATP usage activity, proportional in a given type of exercise to power output, on the duration of exercise until exhaustion, at least for duration times less than ~10 min. Within the computer model used, the continuous increase in cytosolic P_i is due to a linear increase in the additional ATP usage as a function of time with a rate proportional to ATP usage activity. The above finding suggests that the P_i-induced fatigue contributes significantly to the hyperbolic power–duration relationship encountered in experimental studies. Therefore, the present study offers a plausible mechanism underlying the (near-)hyperbolic shape of the power–duration relationship. No such mechanism had been postulated previously in the literature.

Study logic

This study is based on the following simple logic. The additional ATP usage (Korzeniewski and Rossiter 2015), which is equivalent to a decreased power-generation efficiency (PO/ATP ratio) and underlies the (slope of the) slow component of the $\dot{V}O_2$ on-kinetics (Jones et al. 2010; Poole et al. 2016), increases linearly with time (Korzeniewski and Rossiter 2015) and ATP usage activity A_{UT} above critical ATP usage activity (A_{UTcrit}) (Korzeniewski 2018a, 2018b). The continuous increase of the additional ATP usage as a

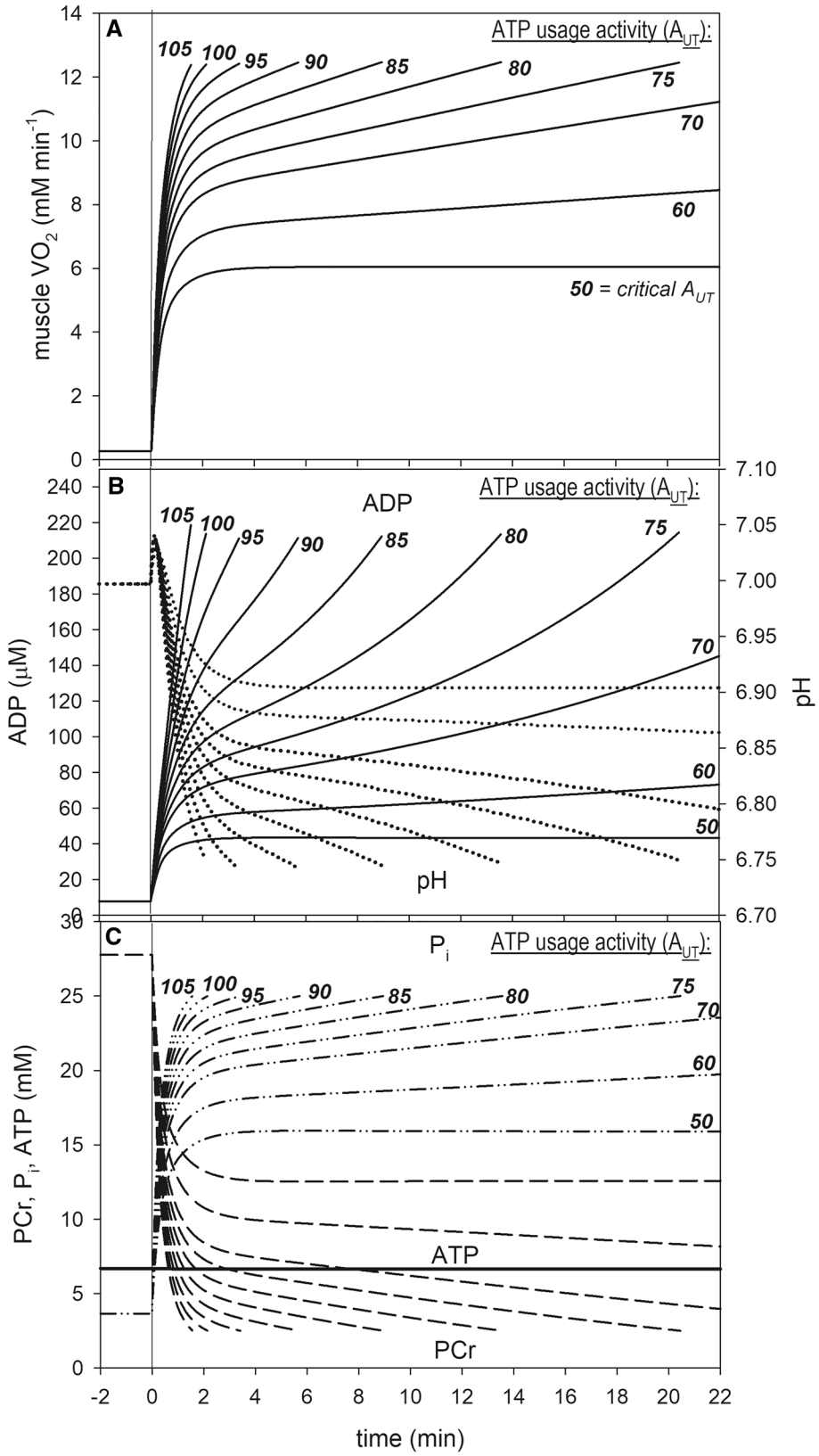

Fig. 2 Simulated muscle $\dot{V}O_2$ and metabolites on-kinetics for various ATP usage activities (A_{UT}) at or above the critical ATP usage activity (A_{UTcrit}). **a** time courses of muscle $\dot{V}O_2$; **b** time courses of cytosolic free ADP and pH; **c** time courses of cytosolic PCr, P_i and ATP. It was assumed that exercise is terminated when P_i exceeds 25 mM

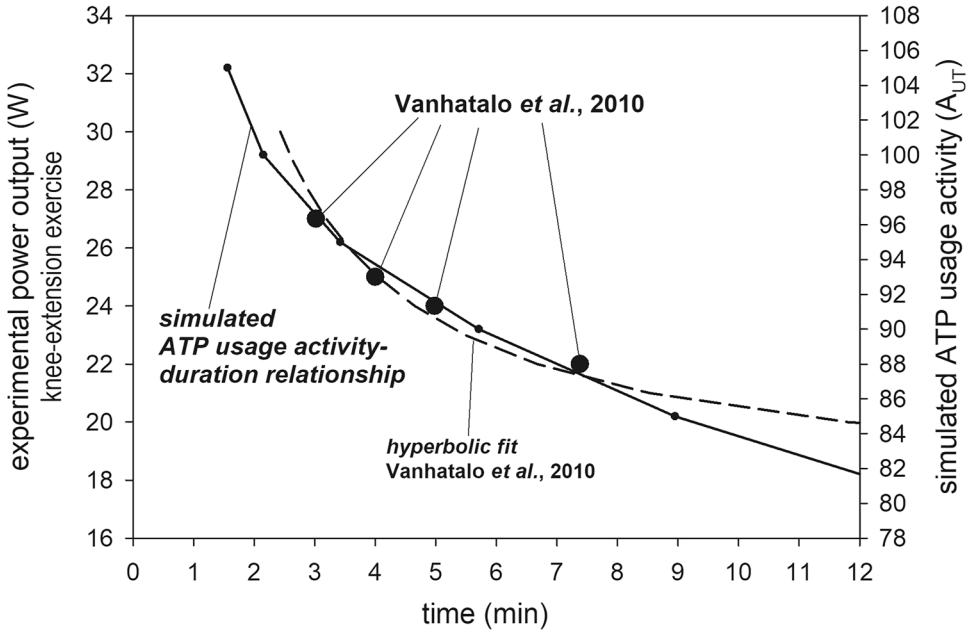

Fig. 3 Comparison of experimental power–duration relationship for knee-extension exercise (points) with simulated relative ATP usage activity (A_{UT})–exercise duration relationship (solid line). The hyperbolic fit of experimental points using the equation parameters given in (Vanhatalo et al. 2010; Fig. 4 a therein) is also presented

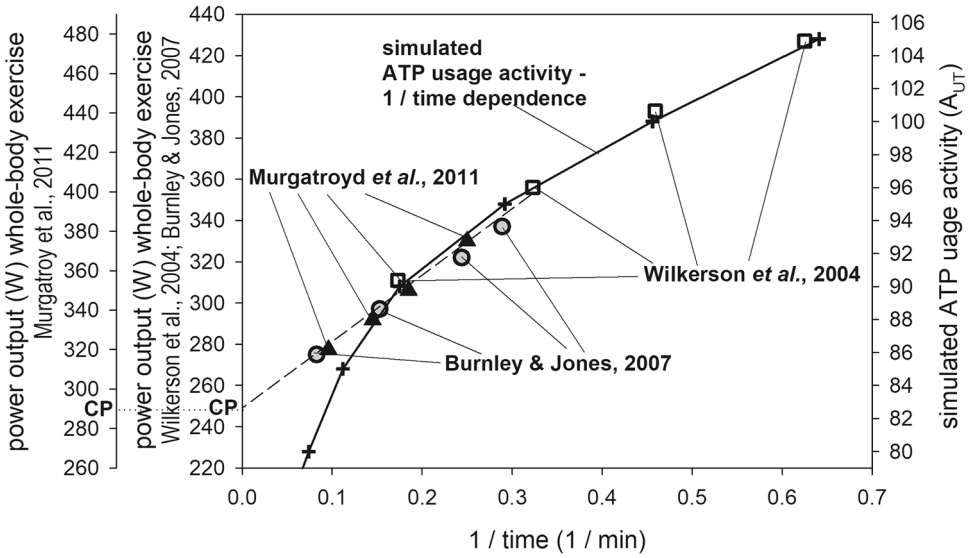

Fig. 4 Comparison of experimental power–1/time (1/duration) relationship for whole-body exercise (cycling) encountered in three studies (points) (left and far left *y* axis) with simulated relative ATP usage activity (A_{UT}) – 1/time (1/duration) relationship (solid line) (right *y* axis). Experimental data were taken from (Wilkerson et al. 2004) and (Burnley and Jones 2007) (left *y* axis) as well as from (Murgatroyd et al. 2011) (far left *y* axis). The dashed line represents a linear extrapolation of the experimental power–duration relationship—its intersection with *y* axis corresponds to critical power (CP)

function of time leads to a continuous increase in the cytosolic P_i level. At the time t_{term}, when P_i exceeds the fixed critical level P_{icrit} (for instance 25 mM used in the present simulations), exercise at a given A_{UT} is terminated because of muscle fatigue. The A_{UT}–t_{term} relationship has a form of a near-hyperbolic ATP usage activity–duration curve, at least for the range of exercise duration of ~ 1.5–10 min. In a given kind of exercise, A_{UT} is proportional to PO, and therefore the ATP usage activity–duration curve corresponds to power–duration curve.

In short: continuous increase in time of additional ATP usage, and thus decrease of PO/ATP (work efficiency), above critical ATP usage activity A_{UTcrit} (ATP usage activity, above which the 'additional' ATP usage appears) proportional to

$A_{UT} - A_{UTcrit} \rightarrow$ continuous increase in $P_i \rightarrow P_i \geq P_{icrit}$ at t_{term} for a given PO $\rightarrow$ termination of exercise (fatigue) $\rightarrow$ ATP usage activity (power)–duration curve.

It should be stressed that the additional ATP usage on principle cannot (there is no possible physical mechanism) directly stimulate $\dot{V}O_2$, and thus cause the slow component of the $\dot{V}O_2$ on-kinetics. On the contrary, it acts exclusively through elevated levels of ADP and P_i: the accelerated ATP hydrolysis causes more intensive ADP and P_i production. This is why the slow component of the $\dot{V}O_2$ on-kinetics starts 'smoothly' in time, whereas the additional ATP usage increases linearly from the very onset of exercise—the further increase in ADP and P_i needs some time and is a little delayed.

Of course, the critical P_i level may vary between different muscles, subjects and exercise types. In fact, when a higher critical P_i, for instance of 27 mM, is assumed, the simulated ATP usage activity–exercise duration relationship becomes even slightly more hyperbolic, as it deviates less and at longer duration times from the hyperbolic shape (not shown).

Confrontation of computer model and simulations with experimental data

The dependence of the intensity of the additional ATP usage on time after the onset of exercise and on ATP usage activity present in Eq. (1) is well supported by a comparison of computer simulations with experimental data. It was shown previously (Korzeniewski and Rossiter 2015) that a linear increase of the additional ATP usage as a function of time gives a good agreement of computer simulations with experimental data. The applied linear dependence of the additional ATP usage on ATP usage activity (parameter, relative rate constant of ATP usage in relation to rest) over critical ATP usage activity ($A_{UT} - A_{UTcrit}$) and on ATP usage flux (v_{UT}) (variable, the rate of ATP usage, see Theoretical Methods) (Eq. 1) also gives a good agreement with experimental data (Murgatroyd et al. 2011)—see Fig. 1. This figure presents the experimental dependence of the speed of the increase of pulmonary $\dot{V}O_2$ (the slope of the slow component of $\dot{V}O_2$) (second derivative of oxygen concentration) (left *y* axis) at the time (t_{term}) of the termination of exercise on power output (lower *x* axis) extracted from (Murgatroyd et al. 2011). This dependence is compared with the simulated dependence of the rate of muscle $\dot{V}O_2$ increase (the slope of the slow component of $\dot{V}O_2$) at the time (t_{term}) of the termination of exercise (dashed line) (far right *y* axis) and ATP usage activity increase (the slope of the 'slow component' of ATP) at the time (t_{term}) of the termination of exercise (solid line) (right *y* axis) on ATP usage activity (A_{UT}) (upper *x* axis). Generally, a good agreement between the simulated dependence of the slope of the $\dot{V}O_2$ and ATP usage slow component at the end of exercise on ATP usage activity and the experimental dependence of the slope of the $\dot{V}O_2$ slow component at the end of exercise on power output can be observed. Therefore, the use of the linear dependence of the additional ATP usage on the ATP usage activity over critical ATP usage activity ($A_{UT} - A_{UTcrit}$) in the present study and previous studies (Korzeniewski 2018a, b) seems fully justified.

The simulated increase in muscle $\dot{V}O_2$ as a function of time for different ATP usage activities (Fig. 2a) was similar to time courses of pulmonary $\dot{V}O_2$ at various power outputs (Murgatroyd et al. 2011; Burnley and Jones 2007; Wilkerson et al. 2004; Özyener et al. 2001; Rossiter 2011; Keir et al. 2018). The simulated muscle $\dot{V}O_2$ that was reached at the end of exercise ($\dot{V}O_{2end}$), terminated because of muscle fatigue, that is, when P_i reached the critical level of 25 mM, was identical for all ATP usage intensities and equaled 12.4 mM min^{-1}. Essentially identical pulmonary $\dot{V}O_{2end}$ for various power outputs was encountered in most experimental studies (Murgatroyd et al. 2011; Burnley and Jones 2007; Özyener et al. 2001; Rossiter 2011; Keir et al. 2018). Nevertheless, in some experimental studies (Wilkerson et al. 2004), pulmonary $\dot{V}O_{2end}$ was somewhat lower for highest power outputs. The last phenomenon can be explained by a significant contribution of anaerobic glycolysis to ATP supply at highest work intensities. Indeed, such an effect can be simulated if a high direct activation (parallel activation) of glycolysis (see e.g., Korzeniewski 2017a) is assumed in the computer model (not shown). The elevated glycolytic ATP supply and lowered $\dot{V}O_{2end}$ can be also caused by O_2 transport limitations (see e.g., Rossiter 2011).

The shape of simulated changes of cytosolic PCr, P_i and pH as a function of time (Fig. 2b,c) agrees well with experimental data (Vanhatalo et al. 2010; Jones et al. 2010). Simulated P_i rose at fatigue 6.8 times in relation to rest (from 3.7 to 25 mM), while it increased about 8 times in (Jones et al. 2008). Simulated PCr dropped to about 9% of the resting value (from 27.7 to 2.5 mM) between rest and fatigue, while it decreases to 5–12% of the resting value in (Vanhatalo et al. 2010) and to about 30% in (Jones et al. 2008). Simulated pH fell (after the initial alkalization) by about 0.25 pH units between rest and fatigue (from 7.0 to 6.75) (this fall was similar, but not identical, for each ATP usage activity), while it dropped by about 0.3 pH units in (Jones et al. 2008) and by 0.32 pH units in (Vanhatalo et al. 2010). A higher (by over 0.5 pH units) decrease in pH was observed using the all-out intermittent isometric single-leg knee-extensor exercise protocol (Broxterman et al., 2018). However, the experimental system used in that study was completely different from the bipedal dynamic constant-power knee-extension exercise system used in the above studies and simulated using a computer model. The drop in pH by about 0.2–0.3 pH units during severe exercise is typical in the latter system—compare also e.g. (Cannon et al., 2014).

Additionally, the simulated end-of-exercise PCr was essentially identical for various ATP usage activities (Fig. 2c), in good agreement with the constancy of PCr at the end of exercises at various power outputs encountered in experimental studies (Vanhatalo et al. 2010). This can imply an also identical end-of-exercise P_i level in real systems, which would agree well with the main assumption of this study concerning the termination of muscle work at a certain critical P_i concentration, although the author is not aware of any such experimental data.

This comparison is limited to ^{31}P MRS data, as these studies are less invasive than biopsy studies.

The simulated dependence of ATP usage activity on exercise duration to exhaustion fits well to experimental points representing the dependence of power output on exercise duration in knee-extension exercise obtained in (Vanhatalo et al. 2010). This is presented in Fig. 3. On the other hand, the simulated curve starts to diverge for exercise durations > ~10 min from the hyperbolic fit of experimental points drawn using the parameter values given in that article for normoxia (Fig. 4 A therein).

The simulated ATP usage activity dependence on the inverse of time to termination of exercise (1/time) also fits quite well to experimental points for the dependence of power output on duration time inverse for whole-body exercise (cycling) obtained in three experimental studies (Murgatroy et al. 2011; Wilkerson et al. 2004; Burnley and Jones 2007). This is demonstrated in Fig. 4. The simulated curve starts to deflect from the straight line fitted to experimental points below 1/time < ~0.12 (time > ~8 min). The most likely reason for this deflection is that for longer exercises factors other than P_i start to predominate in shaping the power–duration relationship.

Generally, the computer simulations carried out under the assumption that muscle work is terminates when cytosolic P_i exceeds the critical value of 25 mM generate a near-hyperbolic dependence of ATP usage on exercise duration that agrees well with experimental data in the range of duration of 1.5–8 (–10) min. For longer duration times the simulated ATP usage activity–exercise duration relationship deviates downwards from the hyperbolic fit of the power–duration relationship to experimental points. Of course, the most likely reason is that P_i is a major fatigue factor only in shorter exercises. Anyway, the theoretical data presented can suggest that critical power estimated from the power–duration relationship is significantly higher, than critical power defined as the power, above which the steady-state of oxygen consumption and metabolite concentrations can be no longer maintained.

P_i as fatigue factor

It has been proposed that elevated P_i is the main peripheral muscle fatigue-inducing factor, with a smaller role played by cytosol acidification and yet smaller by other factors (Allen et al. 2008; Allen and Westerblad 2001; Westerblad et al. 2002; Millar and Homshere 1990; Grassi et al. 2015). Nevertheless, this conclusion meets some problems.

First, in skinned muscle fibers, external P_i starts to diminish external Ca^{2+}-induced muscle tension already at concentrations around, or even lower than, 1 mM (Millar and Honshere 1990; Fryer et al. 1995). However, the system used in those studies with constant external Ca^{2+} was very unphysiological, as it did not involve Ca^{2+} handling and ATP usage by Ca^{2+}-ATPase (SERCA). Therefore, here the effect of P_i constitutes rather a qualitative cue, and not a quantitative measure. On the other hand, intact myocytes with functional Ca^{2+} handling and working Ca^{2+}-ATPase were used in most studies concerning the impact of P_i on muscle fatigue (Allen et al. 2008; Allen and Westerblad 2001; Westerblad et al. 2002). Second, it has been shown that elevated H^+ strongly inhibits Ca^{2+}-ATPase (Wolosker et al. 1997), and therefore cytosol acidification should not be neglected as the factor underlying muscle fatigue and additional ATP usage (see next sub-section). In fact, similar end-exercise H^+ level were simulated (Fig. 2b), and therefore an assumption of H^+ as the exhaustion-causing factor would also result in a near-hyperbolic ATP usage activity–duration relationship. Third, during muscle work, P_i, after the initial quick rise, increases with a moderate or slow pace (Fig. 2c; Jones et al. 2008; Cieslar and Dobson 2000) and therefore slowly approaches the assumed critical P_i value. For this reason, one could wonder why just a minute exceeding of the critical P_i value should cause such a 'sharp' effect as muscle work termination. Nevertheless, various possible effects of P_i have been postulated, namely inhibition of cross-bridge formation, decrease in the myofibrillar Ca^{2+} sensitivity and Ca^{2+} ions precipitation within sarcoplasmic reticulum (SR) (Allen et al. 2008). According to the last mechanism (Allen et al. 2008; Allen and Westerblad 2001), a small further relative increase in P_i could lead to a complete depletion of remaining free Ca^{2+} ions that constitute the signal for muscle contraction, and thus unable cross-bridge formation and force generation. Generally all the enumerated mechanisms of P_i-mediated fatigue can act synergistically and involve reciprocal self-driving relations between P_i rise and ATP usage system.

Nevertheless, the present study does not imply that P_i is the only or even dominating factor responsible for muscle fatigue and voluntary exercise termination. Other factors/mechanisms, both peripheral, especially H^+ in short-duration exercises and depletion of glycogen stores in long-duration exercises, as well as central (Gandevia 2001) should be considered. It is likely that several factors, metabolites, H^+ and others, co-contribute to muscle fatigue. On the other hand, the central neural fatigue mechanisms are likely to sense somehow the metabolic state of working muscles and blood

(e.g., pH and lactate), and react appropriately by inhibition of neural stimulation of already peripherally fatigued muscles. In such a case, the primary source of fatigue would be in both cases located within working muscles (and blood), which would generate direct (peripheral) and indirect (central) fatigue signals terminating muscle work and thus preventing possible damage of already-fatigued muscles.

Causes of additional ATP usage

In the computer model used for simulations it is assumed that the slow component of the $\dot{V}O_2$ and metabolites on-kinetics is underlain by a linear increase of the additional ATP usage with time. Therefore, it is assumed that the decrease of the muscle work efficiency PO/O_2 is caused by a decrease in the efficiency of power generation: PO/ATP, and not of oxidative ATP synthesis: ATP/O_2. It was proposed that while the contribution of the proton leak through the inner mitochondrial membrane, the main candidate for the factor decreasing ATP/O_2, to oxygen consumption can be huge (> 60%) at rest, it is very tiny (1–3%) during intense exercise (Korzeniewski, 2017b). This fact points to the additional ATP usage as the main mechanism of the increase in the $\dot{V}O_2$/PO ratio.

Several various reasons of the appearance of the additional ATP usage above critical ATP usage activity (critical power) are possible. This can be for instance a decrease in the actomyosin-ATPase efficiency (increase in the mechanistic ATP/PO ratio) caused potentially by the fact that at lower phosphorylation potential values the myosin head moves by a shorter distance along the actin filament during a single power stroke driven by one ATP molecule hydrolysis, increase in biomechanical resistance related e.g., to friction of particular working limbs/muscles elements or increase in the contribution of Ca^{2+}-ATPase to ATP usage. The last possibility is supported by the finding that the contribution of Ca^{2+}-ATPase to ATP usage is higher, and thus of power-generating actomyosin-ATPase lower, in fatigue-susceptible type II muscle fibers than in fatigue-resistant type I muscle fibers (Szentesi et al. 2001). However, this does not imply that the slow component is underlain by the type II fibers recruitment, but only suggests that the contribution of calcium pumping to ATP usage can increase with time as the working muscle becomes progressively fatigued. Indeed, some experiments suggest that the slow component, or slow-component-like phenomenon, is still present when there is no additional recruitment of type II fibers (Zoladz et al., 2008; Vanhatalo et al., 2011).

Study limitations

Certainly, the taking into account in computer simulations of only one fatigue factor—P_i—constitutes a significant simplification. However, the present study is not intended to prove that P_i is the only relevant factor, but only to support the idea (Allen et al. 2008) that it is one of major factors/mechanisms responsible for work termination because of fatigue, especially in intense and shortly-lasting exercises. This is made by showing that the assumption that exercise is terminated because of fatigue when P_i reaches the critical value leads to a (near-)hyperbolic power–duration relationship encountered in experimental studies (Jones et al. 2010; Poole et al. 2016).

A constant muscle oxygen concentration of 30 μM was assumed in computer simulations and therefore the possible decrease in O_2 during exercise due to oxygen supply limitations is not taken into account. This is certainly a certain approximation. On the other hand, the muscle O_2 concentration of ~ 60 μM at $\dot{V}O_{2max}$ in normoxia was reported (Roca et al. 1992). Both values are much higher, than the K_m value of oxidative phosphorylation for oxygen, which is significantly lower than 1 μM (Gneiger et al. 1995).

No AMP deamination was assumed in the present computer simulations, as the dependence of this process intensity on power output is not known, and therefore ATP concentration remained essentially constant, while it can drop significantly during intense muscle work (see e.g., Broxterman et al. 2018). The effect of AMP deamination on metabolite levels and $\dot{V}O_2$ during intense constant-power exercise was simulated previously (Korzeniewski 2006). Essentially no effect on $\dot{V}O_2$ was observed. While this process can affect quite significantly ATP (decreases during exercise) and ADP (increases less during exercise), its effect on P_i (increases more), pH (decreases less) and PCr (almost no effect) is rather moderate. Additionally, in lower-intensity constant-power exercises AMP deamination does not occur or is very slow, while in higher-intensity constant-power exercises it has little time to develop. Nevertheless, involving AMP deamination could slightly flatten the simulated power–duration relationship shown in Fig. 3—at higher power outputs the critical P_i level would be reached and exercise would be terminated a little earlier. However, this effect would be small and the power–duration relationship would remain nearly-hyperbolic.

It was suggested that muscle fatigue correlates better with $H_2PO_4^-$, than with pH (Wilson et al. 1985). The level of $H_2PO_4^-$ is a function of total P_i and pH: a drop in pH increases the fraction of P_i being in the form of $H_2PO_4^-$. Therefore, the $H_2PO_4^-$ level involves implicitly the H^+ level. If $H_2PO_4^-$, instead of total P_i, were assumed as the exercise-terminating factor (this would be equivalent to a co-action of total P_i and pH), the power–duration relationship would become a little more flat (the $H_2PO_4^-$ increase would be caused by both total P_i increase and pH decrease), but would remain near-hyperbolic (simulations not shown).

For glucose as respiratory substrate, the real fixed intramitochondrial NADH: $FADH_2$ stoichiometry is 4: 1. For simplicity, it is assumed within the model that 5 NADH, instead of 4 NADH plus 1 $FADH_2$ are produced within mitochondria (the model lacks $FADH_2$ and complex II). As 10 protons are pumped per 2 electrons flowing from NADH to O_2 (by complexes I, III and IV), while only 6 protons are pumped, when electrons flow from $FADH_2$ to O_2 (only complexes III and IV), the overall balance is as follows: 50 protons per 5 NADH in the model and 46 protons per 4 NADH + 1 $FADH_2$ in reality. Therefore, the difference is only 8% and, what is most important, it is constant during exercise (there is no 'side influx' of $FADH_2$). The same concerns the amount of ATP produced per 2 electrons or one O_2 molecule consumed. For this reason, the P/O ratio is slightly greater in the model, than in reality. However, again, it is constant during exercise, while relative changes matter most. Therefore, the discussed simplification has only a negligible impact on the main conclusions drawn in the present study.

Computer simulations reproduce well the experimentally measured power–duration relationship for exercise duration < ~ 10 min. On the other hand, the simulated relationship between ATP usage activity (A_{UT}) and duration time begins to deviate from the hyperbolic dependence fitted to experimental points for end-exercise time longer than 10 min. Of course, the first reason can be that the model used, in particular the assumption of exercise termination at critical P_i and the dependence of the additional ATP usage on power output, is oversimplified, especially for longer exercise durations. Second, indeed other fatigue factors/mechanisms such as cytosol acidification, glycogen depletion or central control can start to predominate in longer exercises. Third, in real systems it can take some time for cytosolic P_i to terminate exercise (e.g., to enter sarcoplasmic reticulum and precipitate with SR Ca^{2+} ions). Fourth, the postulated (near-)hyperbolic power–duration relationship is based mostly on experimental data involving exercises lasting about 2–12 min (Jones et al. 2010; Poole et al. 2016), and may not hold for lower-intensity exercises with longer duration times.

Nevertheless, the general conclusion of this study that cytosolic P_i accumulation can significantly contribute to the near-hyperbolic power–duration relationship seems still valid.

Conclusions

The present theoretical study combines three ideas proposed in earlier articles by other authors: (1) that there exists a critical power (CP), above which no steady state in $\dot{V}O_2$, cytosolic metabolite concentrations and pH can be achieved in voluntary constant-power exercise (Jones et al. 2010; Poole et al. 2016); (2) that muscle fatigue is related to decreased exercise efficiency ($\dot{V}O_2$/ATP ratio) (Grassi et al. 2015); and (3) that P_i (inorganic phosphate) is a major fatigue-related metabolite (Allen et al. 2008). Computer simulations, carried out under the assumption that skeletal muscle work terminates when the cytosolic P_i (inorganic phosphate) exceeds a certain critical value (25 mM in this study) result in a fourth previously-published idea: 4. that a hyperbolic power–duration curve describes the dependence of power output (PO) on the duration time of voluntary constant-power exercise at a given PO (Jones et al. 2010; Poole et al. 2016). This does not imply that cytosolic P_i is the only, or even the main fatigue factor—other factors/mechanisms, for instance cytosol acidification, glycogen stores depletion and central fatigue should be considered. Nevertheless, the present study suggests that P_i is an important factor contributing to muscle fatigue and (near-)hyperbolic shape of the power–duration relationship, at least for exercise duration of ~ 1–10 min. Generally, the present study offers a potential mechanism underlying the hyperbolic shape of the power–duration relationship. No such mechanism had been previously proposed in the literature.

Funding No specific funding was received.

Compliance with ethical standards

Conflict of interest The authors declare that they have no competing interests.

Appendix: Kinetic description of the dynamic model of the skeletal muscle cell bioenergetic system

Subscripts: e, external (cytosolic); i, internal (mitochondrial); t, total; f, free; m, magnesium complex; j, monovalent.

All metabolite concentrations in μM. All rates/fluxes in μM min^{-1}.

DH, NADH supply; C1, complex I; C3, complex III; C4, complex IV; SN, ATP synthase; EX, ATP/ADP carrier; PI, P_i carrier; UT, ATP usage; LK, proton leak; CK, creatine kinase; AK, adenylate kinase; GL, glycolysis; EF, proton efflux/influx to/from blood.

Constants

$k_{DH} = 28{,}074$ μM min^{-1}

$K_{mN} = 100$

$p_D = 0.8$

$k_{C1} = 238.95$ μM mV^{-1} min^{-1}

$k_{C3} = 136.41$ μM mV^{-1} min^{-1}

$k_{C4} = 3.600$ μM^{-1} min^{-1}

$K_{mO} = 120$ μM (mechanistic K_m for O_2, much higher than apparent $K_m \leq 1$ μM)

$k_{SN} = 34{,}317$ μM min^{-1}

$n_A = 2.5$ (phenomenological H^+/ATP stoichiometry of ATP synthase)
$k_{EX} = 54{,}573\ \mu M\ min^{-1}$
$K_{mADP} = 3.5\ \mu M$
$k_{PI} = 69.421\ \mu M^{-1}\ min^{-1}$
$k_{UT} = 781.97\ \mu M\ min^{-1} * A_{UT}$
$A_{UT} = 1$ (rest)
$A_{UT} = > 1–105$ (work of different intensity)
$K_{mA} = 150\ \mu M$
$k_{LK1} = 2.500\ \mu M\ min^{-1}$
$k_{LK2} = 0.038\ mV-1$
$k_{fAK} = 862.10\ \mu M^{-1}\ min^{-1}$
$k_{bAK} = 22.747\ \mu M^{-1}\ min^{-1}$
$k_{fCK} = 1.9258\ \mu M^{-2}\ min^{-1}$
$k_{bCK} = 0.00087538\ \mu M^{-1}\ min^{-1}$
$k_{EF} = 10{,}000\ \mu M\ min^{-1}$
$pH_0 = 7.0$
$k_{GL} = 17.4\ min^{-1}$
$H_{rest}^{+} = 0.1\ \mu M$
$k_{DTe} = 24\ \mu M$ (magnesium dissociation constant for external ATP)
$k_{DDe} = 347\ \mu M$ (magnesium dissociation constant for external ADP)
$k_{DTi} = 17\ \mu M$ (magnesium dissociation constant for internal ATP)
$k_{DDi} = 282\ \mu M$ (magnesium dissociation constant for internal ADP)
$Rc_m = 15$ (cell volume/mitochondria volume ratio)
$B_N = 5$ (buffering capacity coefficient for NAD)
$T = 298$ K
$R = 0.0083$ kJ mol^{-1} K^{-1}
$F = 0.0965$ kJ mol^{-1} mV^{-1}
$S = 2.303 * R * T$
$Z = 2.303 * R * T/F$
$u = 0.861$ ($= \Delta\Psi/\Delta p$)
$c_{buffi} = 0.022$ M H^+/pH unit (buffering capacity for H^+ in matrix)
$c_{buffe} = 0.025$ M H^+/pH unit (buffering capacity for H^+ in cytosol)
$pK_a = 6.8$
$\Delta G_{P0} = 31.9$ kJ mol^{-1}
$E_{mN0} = -320$ mV
$E_{mU0} = 85$ mV
$E_{mc0} = 250$ mV
$E_{ma0} = 540$ mV

Constant metabolite concentrations

$O_2 = 30\ \mu M$
$c_t = 270\ \mu M$ ($= c^{2+} + c^{3+}$, total concentration of cytochrome c)
$U_t = 1350\ \mu M$ ($= UQH_2 + UQ$, total concentration of ubiquinone)
$N_t = 2970\ \mu M$ ($= NADH + NAD^+$, total concentration of NAD)
$a_t = 135\ \mu M$ ($= a^{2+} + c^{3+}$, total concentration of cytochrome a_3)
$Mg_{fe} = 4000\ \mu M$ (free external magnesium concentration)
$Mg_{fi} = 380\ \mu M$ (free internal magnesium concentration)
$A_{iSUM} = 16{,}260\ \mu M$ ($= ATP_{ti} + ADP_{ti}$, total internal adenine nucleotide concentration)
$A_{eSUM} = 6700\ \mu M$ ($= ATP_{te} + ADP_{te} + AMP_e$, total external adenine nucleotide concentration)
$C_{SUM} = 35{,}000\ \mu M$ ($= Cr + PCr$, total creatine concentration)

Values of independent variables, respiration rate (v_{C4}) and AMP_e at rest

$v_{C4} = 267\ \mu M\ min^{-1}$
$NADH = 1735.2\ \mu M$
$UQH_2 = 1212.4\ \mu M$
$c^{2+} = 75.35\ \mu M$
$O_2 = 30.0\ \mu M$
$ATPti = 12{,}833$
$Pi_{ti} = 18{,}666\ \mu M$
$H_i = 0.03757\ \mu M$
$ATP_{te} = 6692.338\ \mu M$
$ADP_{te} = 7.87\ \mu M$
($AMP_e = 0.0259\ \mu M$)
$Pi_{te} = 3653.8\ \mu M$
$PCr = 27{,}768\ \mu M$
$H_e = 0.1000\ \mu M$

Calculations

$c^{3+} = c_t - c^{2+}$
$UQ = U_t - UQH_2$
$NAD^+ = N_t - NADH$
$Cr = C_{SUM} - PCr$
$AMP_e = A_{eSUM} - ATP_{te} - ADP_{te}$
$ADP_{ti} = A_{iSUM} - ATP_{ti}$
$ATP_{fe} = ATP_{te}/(1 + Mg_{fe}/k_{DTe})$
$ATP_{me} = ATP_{te} - ATP_{fe}$
$ADP_{fe} = ADP_{te}/(1 + Mg_{fe}/k_{DDe})$
$ADP_{me} = ADP_{te} - ADP_{fe}$
$ATP_{fi} = ATP_{ti}/(1 + Mg_{fi}/k_{DTi})$
$ATPmi = ATP_{ti} - ATP_{fi}$
$ADP_{fi} = ADP_{ti}/(1 + Mg_{fi}/k_{DDi})$
$ADP_{mi} = ADP_{ti} - ADP_{fi}$
$pH_i = -\log(H_i/10^6)$ (H_i expressed in μM)
$pH_e = -\log(H_e/10^6)$ (H_e expressed in μM)
$\Delta pH\ (mV) = Z\ (pH_i - pH_e)$
$\Delta p\ (mV) = 1/(1 - u)\ \Delta pH$
$\Delta\ \Psi\ (mV) = -(\Delta p - \Delta pH)$
$\Psi_i\ (mV) = 0.65 * \Delta\Psi$
$\Psi_e\ (mV) = -0.35 * \Delta\Psi$
$c_{0i} = (10^{-pHi} - 10^{-pHi-dpH})/dpH$ ('natural' buffering capacity for H^+ in matrix)
$dpH = 0.001$
$r_{buffi} = c_{buffi}/c_{0i}$ (buffering capacity coefficient for H^+ in matrix)

$c_{0e} = (10^{-pHe} - 10^{-pHe-dpH})/dpH$ ('natural' buffering capacity for H^+ in cytosol)

$dpH = 0.001$

$r_{buffe} = c_{buffe}/c_{0e}$ (buffering capacity coefficient for H^+ in cytosol)

$Pi_{je} = Pi_{te}/(1 + 10^{pHe-pKa})$

$Pi_{ji} = Pi_{ti}/(1 + 10^{pHi-pKa})$

$\Delta G_{SN} = n_{A*}\Delta p - \Delta G_P$ (thermodynamic span of ATP synthase)

$\Delta G_P = \Delta G_{P0}/F + Z * \log(10^6 * ATP_{ti}/(ADP_{ti} * Pi_{ti}))$ (concentrations expressed in µM)

$E_{mN} = E_{mN0} + Z/2 * \log(NAD^+/NADH)$ (NAD redox potential)

$E_{mU} = E_{mU0} + Z/2 * \log(UQ/UQH_2)$ (ubiquinone redox potential)

$E_{mc} = E_{mc0} + Z * \log(c^{3+}/c^{2+})$ (cytochrome *c* redox potential)

$E_{ma} = E_{mc} + \Delta p_*(2 + 2u)/2$ (cytochrome a_3 redox potential)

$A_{3/2} = 10^{(Ema-Ema0)/Z}$ (a^{3+}/a^{2+} ratio)

$a^{2+} = a_t/(1 + A_{3/2})$ (concentration of reduced cytochrome a_3)

$\Delta G_{C1} = E_{mU} - E_{mN} - \Delta p_* 4/2$ (thermodynamic span of complex I)

$\Delta G_{C3} = E_{mc} - E_{mU} - \Delta p_*(4 - 2u)/2$ (thermodynamic span of complex III)

$s = 0.7 - (pH\text{-}6.0)*0.5$ (net stoichiometry of proton consumption/production by creatine kinase when coupled with ATP consumption/production, respectively; Lohman reaction).

Kinetic equations

Substrate dehydrogenation: $v_{DH} = k_{DH} \frac{1}{\left(1 + \frac{K_{mN}}{NAD^+/NADH}\right)^{p_D}}$

Complex I: $v_{C1} = k_{C1} \cdot \Delta G_{C1}$

Complex III: $v_{C3} = k_{C3} \cdot \Delta G_{C3}$

Complex IV: $v_{C4} = k_{C4} \cdot a^{2+} \cdot c^{2+} \frac{1}{1 + \frac{K_{mO}}{O_2}}$

ATP synthase: $v_{SN} = k_{SN} \frac{\gamma - 1}{\gamma + 1}, \gamma = 10^{\Delta G_{SN}/Z}$

ATP/ADP carrier

$$\dot{v}_{EX} = k_{EX} \cdot \left(\frac{ADP_{fe}}{ADP_{fe} + ATP_{fe} \cdot 10^{-\Psi_e/Z}} - \frac{ADP_{fi}}{ADP_{fi} + ATP_{fi} \cdot 10^{-\Psi_i/Z}}\right) \cdot \left(\frac{1}{1 + K_{mADP}/ADP_{fe}}\right)$$

Phosphate carrier: $v_{PI} = k_{PI} \cdot \left(Pi_{je} \cdot H_e - Pi_{ji} \cdot H_i\right)$

ATP usage: $v_{UT} = k_{UT} \frac{1}{1 + \frac{K_{mA}}{ATP_{te}}}$

Proton leak: $v_{LK} = k_{LK1} \cdot \left(e^{k_{LK2} \cdot \Delta p} - 1\right)$

Adenylate kinase:

$v_{AK} = k_{fAK} \cdot ADP_{fe} \cdot ADP_{me} - k_{bAK} \cdot ATP_{me} \cdot AMP_e$

Creatine kinase:

$v_{CK} = k_{fCK} \cdot ADP_{te} \cdot PCr \cdot H_e^+ - k_{bCK} \cdot ATP_{te} \cdot Cr$

Proton efflux: $v_{EF} = k_{EF} \cdot \left(pH_0 - pH_e\right)$

Glycolysis: $v_{GL} = k_{GL} \cdot \left(ADP_{te} + AMP_e\right)\left(H^+_{rest}/H^+\right)^3$ (anaerobic glycolysis present) or $v_{GL} = 0.2 \cdot v_{DH}$ (anaerobic glycolysis absent)

Set of differential equations

$\dot{NADH} = \left(v_{DH} - v_{C1}\right) \cdot R_{cm}/B_N$

$\dot{UQH}_2 = \left(v_{C1} - v_{C3}\right) \cdot R_{cm}$

$\dot{c}^{2+} = \left(v_{C3} - 2 \cdot v_{C4}\right) \cdot 2 \cdot R_{cm}$

$\dot{O}_2 = 0$ (constant saturated oxygen concentration = 30 µM) or $\dot{O}_2 = -v_{C4}$

$\dot{H}_i^+ = -\left(2 \cdot (2 + 2 \cdot u) \cdot v_{C4} + (4 - 2 \cdot u) \cdot v_{C3} + 4 \cdot v_{C1} - n_A \cdot v_{SN} - u \cdot v_{EX} - (1 - u) \cdot v_{PI} - v_{LK}\right) \cdot R_{cm}/r_{buffi}$

$\dot{ATP}_{ti} = \left(v_{SN} - v_{EX}\right) \cdot R_{cm}$

$\dot{Pi}_{ti} = \left(v_{PI} - v_{SN}\right) \cdot R_{cm}$

$\dot{ATP}_{te} = \left(v_{EX} - v_{UT} + v_{AK} + v_{CK} + 1.5 \cdot v_{GL}\right) \cdot R_{cm}/\left(R_{cm} - 1\right)$

$\dot{ADP}_{te} = \left(v_{UT} - v_{EX} - 2 \cdot v_{AK} - v_{CK} - 1.5 \cdot v_{GL}\right) \cdot R_{cm}/\left(R_{cm} - 1\right)$

$\dot{Pi}_{te} = \left(v_{UT} - v_{PI} - 1.5 \cdot v_{GL}\right) \cdot R_{cm}/\left(R_{cm} - 1\right)$

$\dot{PCr} = -v_{CK} \cdot R_{cm}/\left(R_{cm} - 1\right)$

$\dot{H}_e^+ = \left(2 \cdot (2 + 2 \cdot u) \cdot v_{C4} + (4 - 2 \cdot u) \cdot v_{C3} + 4 \cdot v_{C1} - n_A \cdot v_{SN} - u \cdot v_{EX} - (1 - u) \cdot v_{PI} - v_{LK} - s \cdot v_{CK} - v_{EF} + v_{GL} - 0.2 \cdot v_{DH}\right)/ r_{buffe} \cdot R_{cm}/\left(R_{cm} - 1\right)$

Simulations of work transitions in electrically and cortically stimulated muscle during constant-power exercise, step-incremental exercise and ramp-incremental exercise

See Korzeniewski (2017a, 2018a, b).

References

Allen DG, Westerblad H (2001) Role of phosphate and calcium stores in muscle fatigue. J Physiol 536:657–665

Allen DG, Lamb GD, Westerblad H (2008) Skeletal muscle fatigue: cellular mechanisms. Physiol Rev 88:287–332

Broxterman RM, Hureau TJ, Layec G, Morgan DE, Bledsoe AD, Jessop JE, Amann M, Richardson RS (2018) Influence of group III/IV muscle afferents on small muscle mass exercise performance: a bioenergetics perspective. J Physiol 596:2301–2314

Burnley M, Jones AM (2007) Oxygen uptake kinetics as a determinant of sports performance. Eur J Sports Science 7:63–79

Cannon DT, Bimson WE, Hampson SA, Bowen TS, Murgatroyd SR, Marwood S, Kemp GJ, Rossiter HB (2014) Skeletal muscle ATP turnover by ^{31}P magnetic resonance spectroscopy during moderate and heavy bilateral knee extension. J Physiol 592:5287–5300

Cieslar JH, Dobson GP (2000) Free [ADP] and aerobic muscle follow at least second order kinetics in rat gastrocnemius in vivo. J Biol Chem 275:6129–6134

Cooke R, Franks K, Luciani GB, Pate E (1988) The inhibition of rabit skeletal muscle contraction by hydrogen ions and phosphate. J Physiol 395:77–97

Enoka RM, Duchateau (2008) Muscle fatigue: what, why and how it influences muscle function. J Physiol 586:11–23

Fryer MW, Owen VJ, Lamb GD, Stephenson DG (1995) Effects of creatine phosphate and P_i on Ca^{2+} movements and tension development in rat skinned skeletal muscle fibers. J Physiol 482:123–140

Gandevia SC (2001) Spinal and supraspinal factors in human muscle fatigue. Physiol Rev 81:1725–1789

Giannesini B, Izquierdo M, Confort-Gouny S, Cozzone PJ, Bendahan D (2001) Time-dependent and indirect effect of inorganic phosphate on force production in rat gastrocnemius exercising muscle determined by ^{31}P-MRS. FEBS Lett 507:25–29

Gnaiger E, Steinlechner-Maran R, Méndez G, Eberl T, Margreiter R (1995) Control of mitochondrial and cellular respiration by oxygen. J Bioenerg Biomembr 27:583–596

Grassi B, Rossiter HB, Zoladz JA (2015) Skeletal muscle fatigue and decreased efficiency: two sides of the same coin? Exerc Sport Sci Rev 43:75–83

Jones AM, Wilkerson DP, DiMenna F, Fulford J, Poole DC (2008) Muscle metabolic responses to exercise above and below the "critical power" assessed using ^{31}P-MRS. Am J Physiol Regul Integr Comp Physiol 294:R585–R593

Jones AM, Vanhatalo A, Burnley M, Morton RH, Poole DC (2010) Critical power: implications for determination of VO_{2max} and exercise tolerance. Med Sci Sports Exerc 42:1876–1890

Jones AM, Grassi B, Christensen B, Krustrup P, Bangsbo J, Poole DC (2011) Slow component of VO_2 kinetics: mechanistic bases and practical applications. Med Sci Sports Exerc 43:2046–2062

Keir DA, Paterson DH, Kowalchuk JM, Murias JM (2018) Using ramp-incremental VO_2 responses for constant-intensity exercise selection. Appl Physiol Nutr Metab 43:882–892

Korzeniewski B (1998) Regulation of ATP supply during muscle contraction: theoretical studies. Biochem J 330:1189–1195

Korzeniewski B (2006) AMP deamination delays muscle acidification during heavy exercise and hypoxia. J Biol Chem 281:3057–3066

Korzeniewski B (2017) Regulation of oxidative phosphorylation through each-step activation (ESA): evidences from computer modeling. Prog Biophys Mol Biol 125:1–23

Korzeniewski B (2018) Regulation of oxidative phosphorylation is different in electrically- and cortically-stimulated skeletal muscle. PLoS ONE 13:e0195620

Korzeniewski B (2018) Muscle VO_2-power output nonlinearity in constant-power, step-incremental, and ramp-incremental exercise: magnitude and underlying mechanisms. Physiol Rep 6:e13915

Korzeniewski B, Liguzinski P (2004) Theoretical studies on the regulation of anaerobic glycolysis and its influence on oxidative phosphorylation in skeletal muscle. Biophys Chem 110:147–169

Korzeniewski B, Rossiter HB (2015) Each-step activation of oxidative phosphorylation is necessary to explain muscle metabolite kinetic responses to exercise and recovery in humans. J Physiol 593:5255–5268

Korzeniewski B, Zoladz JA (2001) A model of oxidative phosphorylation in mammalian skeletal muscle. Biophys Chem 92:17–34

Korzeniewski B (2017b) Contribution of proton leak to oxygen consumption in skeletal muscle during intense exercise is very low despite large contribution at rest. PLoS One 12:e.0185991

Millar NC, Homsher E (1990) The effect of phosphate and calcium on force generation in glycerinated rabbit skeletal muscle fibers. J Biol Chem 265:20234–20240

Murgatroyd SR, Ferguson C, Ward SA, Whipp BJ, Rossiter HB (2011) Pulmonary O_2 uptake kinetics as a determinant of high-intensity exercise tolerance in humans. J Appl Physiol 110:1598–1606

Özyener F, Rossiter HB, Ward SA, Whipp BJ (2001) Influence of exercise intensity on the on- and off-transient kinetics of pulmonary oxygen uptake in humans. J Physiol 533:891–902

Poole DC, Ward SA, Gardner GW, Whipp BJ (1988) Metabolic and respiratory profile of the upper limit for prolonged exercise in man. Ergonomics 31:1265–1279

Poole DC, Burnley M, Vanhatalo A, Rossiter HB, Jones AM (2016) Critical power: an important fatigue threshold in exercise physiology. Med Sci Sports Exerc 48:2320–2334

Roca J, Agusti AGN, Alonso A, Poole DC, Viegas C, Barbera JA, Rodriguez-Roisin R, Ferrer A, Wagner PD (1992) Effects of training on muscle O_2 transport at VO_{2max}. J Appl Physiol 73:1067–1076

Rossiter HB (2011) Exercise: Kinetic considerations for gas exchange. Compr Physiol 1:203–244

Rossiter HB, Ward SA, Kowalchuk JM, Howe FA, Griffiths JR, Whipp BJ (2002) Dynamic asymmetry of phosphocreatine concentration and O_2 uptake between the on- and off-transients of moderate- and high-intensity exercise in humans. J Physiol 541:991–1002

Szantesi P, Zaremba R, van Mechelen W, Stienen JM (2001) ATP utilization for calcium uptake and force production in different types of human skeletal muscle fibres. J Physiol 531:393–403

Vanhatalo A, Fulford J, DiMenna FJ, Jones AM (2010) Influence of hyperoxia on muscle metabolic responses and the power–duration relationship during severe-intensity exercise in humans: a ^{31}P magnetic resonance spectroscopy study. Exp Physiol 95:528–540

Vanhatalo A, Poole DC, DiMenna FJ, Bailey SJ, Jones AM (2011) Muscle fiber recruitment and the slow component of O_2 uptake: constant work rate vs. all-out sprint exercise. Am J Physiol Regul Integr Comp Physiol 300:R700–707

Wan J-j, Quin Z, Wang P-y, Liu X (2017) Muscle fatigue: general understanding and treatment. Exp Mol Med 49:e384. https://doi.org/10.1038/emm.2017.194

Westerblad H, Allen DG, Lännergren J (2002) Muscle fatigue: lactic acid or inorganic phosphate the major cose? News Physiol Sci 17:17–21

Wilkerson DP, Koppo K, Barstow TJ, Jones AM (2004) Effect of work rate on the functional 'gain' of Phase II pulmonary O_2 uptake response to exercise. Resp Physiol Neurobiol 142:211–223

Wilson JR, McCully KK, Mancini DM, Boden B, Chance B (1988) Relationship of muscular fatigue to pH and diprotonated P_i in humans: a ^{31}P-NMR study. J Appl Physiol 64:2333–2339

Wolosker H, Rocha JB, Engelender S, Panizzutti R, De Miranda J, de Meis L (1997) Sarco/endoplasmic reticulum Ca^{2+}-ATPase isoforms: diverse responses to acidosis Biochem J 321:545–550.

Zoladz JA, Gladden LB, Hogan MC, Nieckarz Z, Grassi B (2008) Progressive recruitment of muscle fibers is not necessary for the slow component of VO_2 on-kinetics. J Appl Physiol 105:575–580